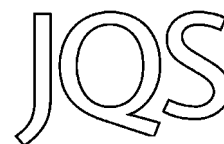


# $^{10}\text{Be}$ and $^{26}\text{Al}$ exposure-age dating of bedrock surfaces on the Aran ridge, Wales: evidence for a thick Welsh Ice Cap at the Last Glacial Maximum



NEIL F. GLASSER,<sup>1\*</sup> PHILIP D. HUGHES,<sup>2</sup> CASSANDRA FENTON,<sup>3,4</sup> CHRISTOPH SCHNABEL<sup>4</sup> and HENRIK ROTHER<sup>5</sup>

<sup>1</sup>Centre for Glaciology, Institute of Geography and Earth Sciences, Aberystwyth University, Aberystwyth SY23 3DB, Wales, UK

<sup>2</sup>Quaternary Environments and Geoarchaeology Research Group, Geography, School of Environment and Development, University of Manchester, Manchester M13 9PL, UK

<sup>3</sup>Helmholtz-Zentrum Potsdam – Deutsches GeoForschungsZentrum, Potsdam, Germany

<sup>4</sup>NERC Cosmogenic Isotope Analysis Facility, SUERC, Scottish Enterprise Technology Park, East Kilbride 975 0QF, Scotland, UK

<sup>5</sup>AMS Laboratory, SUERC, Scottish Enterprise Technology Park, East Kilbride 975 0QF, Scotland, UK

Received 19 January 2011; Revised 19 April 2011; Accepted 27 April 2011

**ABSTRACT:** This paper presents results of the analysis of paired cosmogenic isotopes ( $^{10}\text{Be}$  and  $^{26}\text{Al}$ ) from eight quartz-rich samples collected from ice-moulded bedrock on the Aran ridge, the highest land in the British Isles south of Snowdon. On the Aran ridge, comprising the summits of Aran Fawddwy (905 m a.s.l.) and Aran Benllyn (885 m a.s.l.),  $^{26}\text{Al}$  and  $^{10}\text{Be}$  ages indicate complete ice coverage and glacial erosion at the global Last Glacial Maximum (LGM). Six samples from the summit ridge above 750–800 m a.s.l. yielded paired  $^{10}\text{Be}$  and  $^{26}\text{Al}$  ages ranging from 17.2 to 34.4 ka, respectively. Four of these samples are very close in age ( $^{10}\text{Be}$  ages of  $17.5 \pm 0.6$ ,  $17.5 \pm 0.7$ ,  $19.7 \pm 0.8$  and  $20.0 \pm 0.7$  ka) and are interpreted as representing the exposure age of the summit ridge. Two other summit samples are much older ( $^{10}\text{Be}$  ages of  $27.5 \pm 1.0$  and  $33.9 \pm 1.2$  ka) and these results may indicate nuclide inheritance. The  $^{26}\text{Al}/^{10}\text{Be}$  ratios for all samples are indistinguishable within one-sigma uncertainty from the production rate ratio line, indicating that there is no evidence for a complex exposure history. These results indicate that the last Welsh Ice Cap was thick enough to completely cover the Aran ridge and achieve glacial erosion at the LGM. However, between c. 20 and 17 ka ridge summits were exposed as nunataks at a time when glacial erosion at lower elevations (below 750–800 m a.s.l.) was achieved by large outlet glaciers in the valleys surrounding the mountains. Copyright © 2011 John Wiley & Sons, Ltd.

**KEYWORDS:** cosmogenic  $^{26}\text{Al}$ ; cosmogenic  $^{10}\text{Be}$ ; British–Irish Ice Sheet; Last Glacial Maximum; Heinrich Event 1; nunatak.

## Introduction

The last British–Irish Ice Sheet (BIIS) comprised several independent ice domes with individual ice divides, spreading centres and ice-flow patterns (Hubbard *et al.*, 2009). Interaction between the individual components of the BIIS was both spatially and temporally variable so that patterns and rates of ice discharge were also variable through time. It is, however, possible to identify two important components of ice discharge that appear to have been long-lived throughout the lifetime of the BIIS (Fig. 1):

1. An Irish Sea Glacier, which flowed southwards from Northern Ireland, south-west Scotland and north-west England, into the south-western and north-eastern part of Wales (e.g. Bowen, 1973; Thomas, 1985; Glasser *et al.*, 2001; O’Cofaigh and Evans, 2001). It has been argued that this ice mass receded rapidly from its maximum position of the last cold stage by iceberg calving in a glacio-isostatically depressed marine basin (Eyles and McCabe, 1989), a view subsequently countered by several workers (e.g. McCarroll, 2001). McCarroll *et al.* (2010) argued that this Irish Sea Glacier failed to reach the Preseli Hills of North Pembrokeshire yet extended southwards to impinge on the northern Isles of Scilly at c. 21 ka. In Anglesey and the Lleyn Peninsula, their cosmogenic surface exposure age dating suggests deglaciation of North-West Wales by c. 23–18 ka.
2. A terrestrially based Welsh Ice Cap, which comprised a semi-independent ice mass with several dispersion centres in the upland areas of North and Mid-Wales (e.g. McCarroll

and Ballantyne, 2000). This ice mass was at times confluent with the Irish Sea Glacier and at times independent of it. During the last cold stage, although the Welsh Ice Cap coalesced with other terrestrial ice caps over the British Isles it remained an independent ice centre (Jansson and Glasser, 2005).

There are, however, a number of uncertainties remaining concerning the nature of the last BIIS and the relationship between its individual flow components (Ballantyne, 2010). For example, very little is known about the nature of the interactions between the Welsh Ice Cap and the Irish Sea Glacier and the dynamic behaviour and palaeoglaciology of the two ice masses. Surface exposure dating using cosmogenic isotopes has been shown to be a very powerful technique for inferring the patterns and timing of former ice-sheet events. Within the UK, it has been used to establish both horizontal and vertical limits of the former BIIS (Bowen *et al.*, 2002; Ballantyne, 2010; McCarroll *et al.*, 2010).

The Last Glacial Maximum (LGM) refers to the period of maximum global ice volume during the last glacial cycle. Yokoyama *et al.* (2000) argued that global land-based ice reached its maximum extent between 21 and 19 ka based on global sea-level minima. However, more recent research on the global sea-level minima places the global ice maximum slightly earlier at between 26 and 21 ka (Peltier and Fairbanks, 2006). Other authors constrain the LGM to 23–19 ka based on a range of multiproxy data (Mix *et al.*, 2001; MARGO Project Members, 2009). The actual definition of the term ‘LGM’ is open to debate depending on what criteria are used to define it. If ice volume alone is considered the main criterion, then the global sea-level research of Peltier and Fairbanks (2006) placing the LGM at 26–

\*Correspondence: N. F. Glasser, as above.  
E-mail: nfg@aber.ac.uk

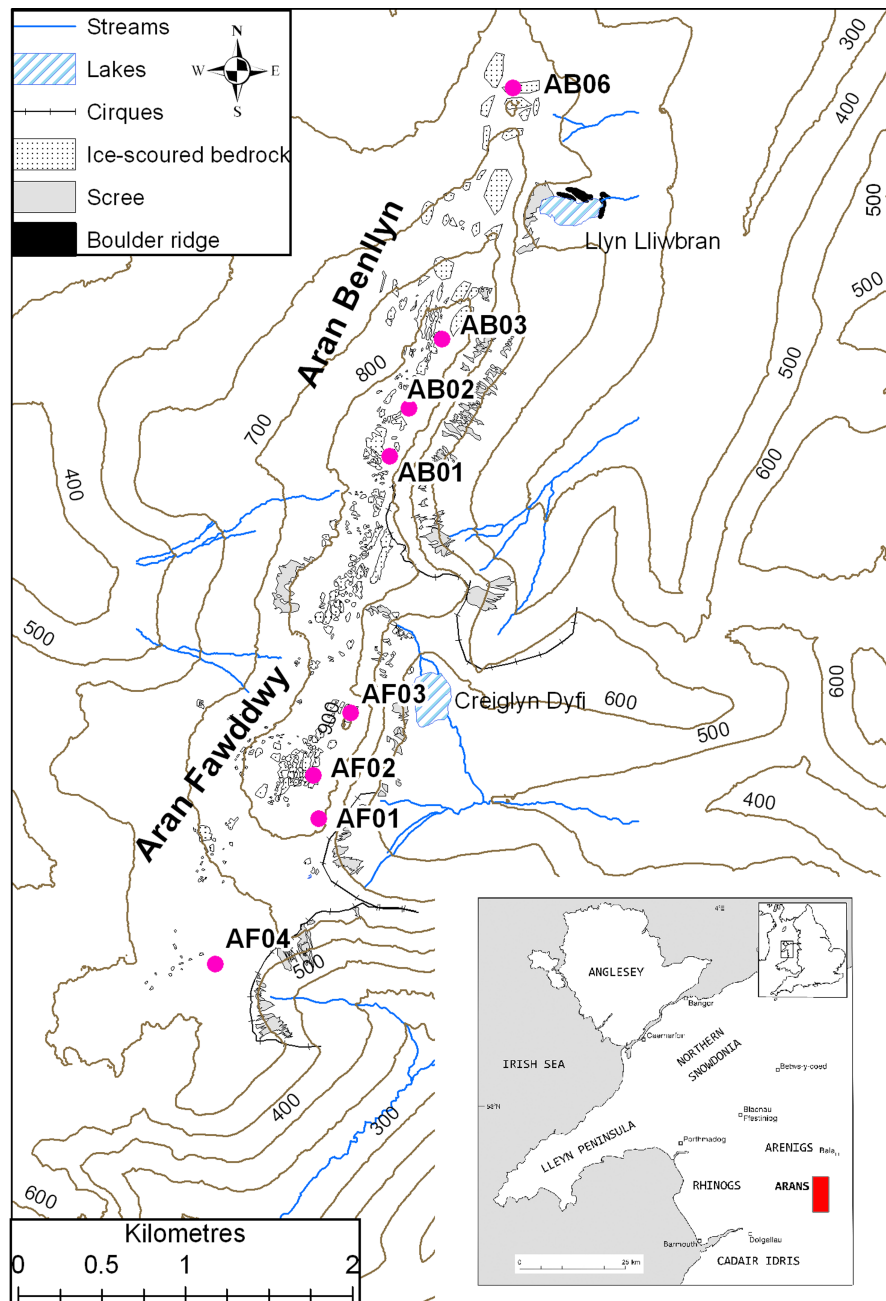


**Figure 1.** Geomorphological map of the Aran Fawddwy and Aran Benllyn area showing the main geomorphological features and sample locations. The map is based on analysis of aerial photography and field mapping. Inset map: location of the study area within Wales and place names mentioned in the text. This figure is available in colour online at [wileyonlinelibrary.com](http://wileyonlinelibrary.com).

21 ka may be the most appropriate – a stance taken by Ballantyne (2010) in his review of the last maximum extent of the BIIS.

Bowen *et al.* (2002) concluded that the BIIS reached its maximum extent during the last cold stage, not at the LGM, but that 'The most extensive Devensian glacial advance was between isotope stage 5e (118 ka) and 37.5 ka' (Bowen *et al.*, 2002, p. 99). Bowen *et al.* (2002) used  $^{36}\text{Cl}$  evidence from erratic boulders and radiocarbon dating in Ireland to infer that the BIIS reached a less extensive LGM position at about 21 ka, soon after Heinrich Event 2. They argued that a cluster of  $^{36}\text{Cl}$  and  $^{14}\text{C}$  ages, at  $21.4 \pm 1.3$  ka, records an initial pulse of deglaciation that was followed by extensive deglaciation at about  $17.4 \pm 0.4$  ka just before Heinrich Event 1 (17–16 ka), when the ice sheet then readvanced. On the basis of these exposure ages, Bowen *et al.* (2002) argued that the BIIS probably existed throughout much of Devensian time as a

mobile and sensitive ice sheet, during which the LGM advance was but one important event.

Ballantyne (2010) reviewed over 160  $^{10}\text{Be}$  and  $^{36}\text{Cl}$  exposure ages relating to the extent and chronology of the last BIIS and concluded that at the LGM the BIIS extended over all low ground in Scotland and all (or almost all) of Ireland. Thus, the large body of evidence presented in Ballantyne (2010) and the works of others, such as O'Cofoigh and Evans (2007), appears to contradict the arguments of Bowen *et al.* (2002) described above. Exposure ages obtained for high-level sites above trimlines on the mountains of north-western Scotland and Ireland pre-date the LGM, suggesting that high plateaux in these areas escaped significant glacial erosion, possibly under a protective cover of cold-based glacier ice that remained frozen to the underlying substrate.

The vertical extent of the Welsh Ice Cap in mountainous areas of Wales is also an area of debate – especially regarding

interpretations about the timing of glacial overriding of the highest summits (Hughes, 2002a, b; McCarroll and Ballantyne, 2002). Hughes (2002a, b) hypothesized that the Arans and Arenigs (Fig. 1) may have stood above the ice cap as nunataks at the LGM and, instead, were overridden by ice at an earlier time. McCarroll and Ballantyne (2002) took an alternative view and argued that the Arans were overridden by ice at the LGM. Hughes based his proposals on the presence of well-developed frost shattering on the summits of both the Arans and neighbouring Arenigs. Similar observations were made in the Arenigs by Fearnside (1905, p. 635) who noted that 'it is uncertain whether or not the highest mountains were ever entirely overridden by ice. Certain it is however, that the highest summits are so much frost-split, that ... all the important hilltops protruded as nunataks'. However, the significance of this evidence in both the Arans and the Arenigs was disputed by McCarroll and Ballantyne (2002). In a response to these authors, Hughes (2002b, p. 17) concluded the debate by stating that 'cosmogenic isotope exposure dating from these summit areas, if possible, would further test the possibility that the summits stood above the last ice sheet'. Here we aim to test the competing hypotheses of Hughes (2002a, b) and of McCarroll and Ballantyne (2002) by using paired  $^{10}\text{Be}$  and  $^{26}\text{Al}$  surface exposure dating of bedrock surfaces on the Aran ridge.

## Study area

Aran Fawddwy (905 m a.s.l.) and Aran Benllyn (885 m a.s.l.), collectively termed here the Arans, are situated in the southern part of Snowdonia National Park (Fig. 1). The Aran ridge runs roughly north-south connecting Aran Fawddwy in the south with Aran Benllyn in the north (Fig. 2). The two summits lie on a c. 4-km-long ridge that is continually above 800 m a.s.l. Aran Fawddwy is the highest summit in the British Isles south of Snowdon (1085 m a.s.l.). The ridge crest and the western slopes

are dominated by Ordovician felsic ash-flow tuffs and associated intrusive and extrusive rhyolites. Quartz veins are widespread within these volcanic rocks. In contrast, the eastern slopes of the Aran ridge are composed of Ordovician mudstones and siltstones (EDINA Geology Digimap, 2009). At least two NE-facing cirques contain moraines, at Llyn Lliwbran and Cwm Cywarch, and these are thought to have contained small glaciers during the Younger Dryas (Hughes, 2002c, 2009). The Arans are ideal for using cosmogenic  $^{10}\text{Be}$  and  $^{26}\text{Al}$  contained in quartz to test competing hypotheses about earlier former vertical ice-sheet dimensions because the mountains are strategically positioned in the centre of Wales and close to the ice divide of the former Welsh Ice Cap (e.g. Greenly, 1919).

## Methods

### *Geomorphological mapping and sample collection*

A geomorphological map of the Aran Fawddwy and Aran Benllyn area was made in ArcMap GIS using 25-cm digital aerial photographs (Figs 1 and 2). Mapped landforms include areas of ice-moulded bedrock, plateau remnants, cirques and major scree slopes. Samples for cosmogenic nuclide surface-exposure ( $^{10}\text{Be}$  and  $^{26}\text{Al}$ ) dating were collected from ice-moulded bedrock landforms in June 2009 following the sampling guidelines of Gosse and Phillips (2001) (Table 1). Quartz-rich samples were collected from the top 5 cm of the bedrock using a hammer and chisel. Detailed site descriptions (e.g. geomorphological context, topographic context and requirement for topographic shielding measurements) were made at each of the localities where samples were collected. The precise locations and altitude of the samples were recorded using a hand-held Garmin GPS and are accurate to  $\pm 4$  m.

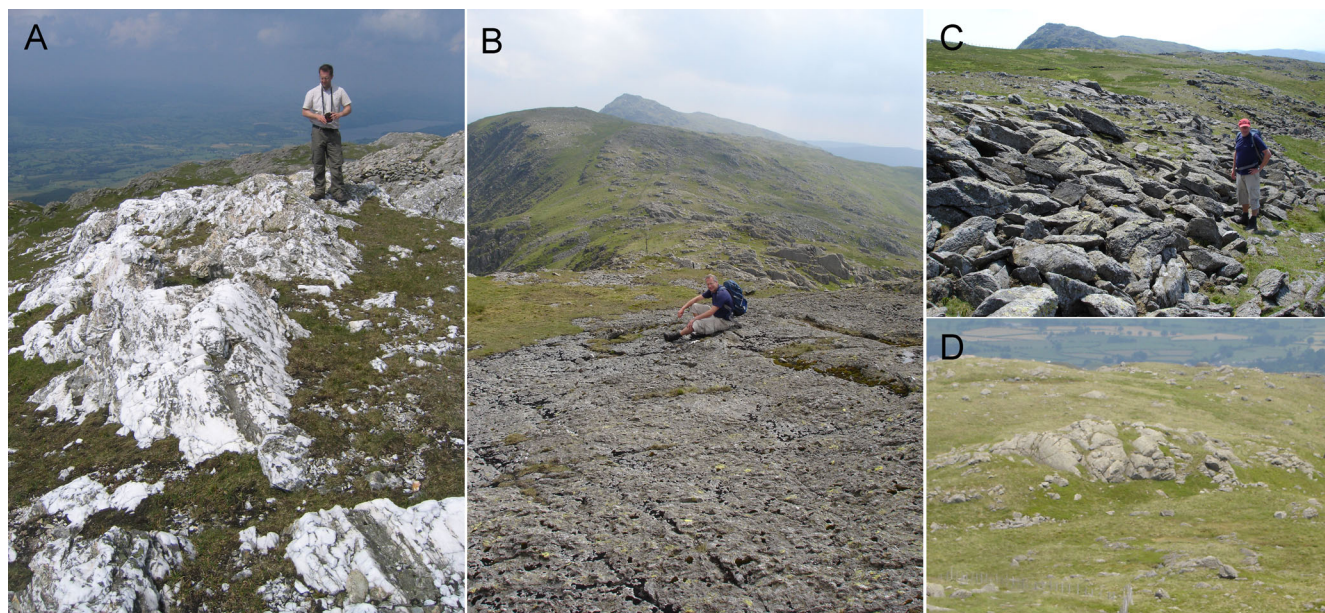


**Figure 2.** (A) Resistant quartz outcrop on the summit of Aran Benllyn. Sample AB02 was taken from this outcrop and yielded paired  $^{10}\text{Be}/^{26}\text{Al}$  ages of 33.4/34.4 ka. This is much older than other samples on the summit ridge and the exposure is interpreted as an anomalously old outlier due to inheritance where ice has been unable to erode to sufficient depth to zero the cosmogenic nuclide signal. (B) Ice-moulded bedrock on the summit ridge of the Arans. This is the site of sample AB01 at an altitude of 878 m a.s.l., which yielded  $^{26}\text{Al}/^{10}\text{Be}$  ages of  $17.5 \pm 0.6/17.2 \pm 0.6$  ka. (C) Example of degraded bedrock near the summit of Aran Benllyn at approximately 850 m a.s.l. Looking south with Aran Fawddwy in the background. This type of bedrock surface is interspersed with ice-moulded bedrock as in B. However, on lower slopes ice-moulded bedrock is more pronounced, as shown in D: example of lower-level ice-moulded bedrock at Moel Ffenigl on the northern end of the Aran Benllyn ridge (600 m a.s.l.), looking north-eastwards. The former ice flow direction was from left to right, from the north-west (note the numerous large glacially transported boulders scattered over this ridge). This figure is available in colour online at [wileyonlinelibrary.com](http://wileyonlinelibrary.com).

**Table 1.** Sample details and context for the eight samples collected and analysed on Aran Fawddwy and Aran Benllyn.

Sample	British grid reference	SUERC AMS- ID	Elevation (m a.s.l.)	Weight (g)	Thickness (cm)
Samples collected from degraded ice-moulded bedrock at sites >750–800 m a.s.l.					
AB01	SH86532401	b4258	878	285	3
AB02	SH86682428	b4261	881	873	6
AB03	SH86922477	b4262	846	716	3
AF01	SH86082178	b4644	818	601	2
AF02	SH85972197	b4264	880	832	6
AF03	SH86212241	b4265	901	753	5
Samples collected from well-preserved ice-moulded bedrock at sites <750–800 m a.s.l.					
AB06	SH87222610	b4642	608	975	3
AF04	SH85482095	b4267	638	975	4

All samples were taken from quartz veins except AB06 which was a quartz-rich rhyolitic vein.

### Cosmogenic $^{10}\text{Be}$ and $^{26}\text{Al}$ dating

Paired cosmogenic  $^{10}\text{Be}$  and  $^{26}\text{Al}$  dating is now commonly and effectively used to infer the ages of former glacial events by dating the ages of moraine boulders and erratic boulders and also by determining the age of glacially eroded bedrock surfaces and related glacial/periglacial/preglacial landforms (Cockburn and Summerfield, 2004). Because of their different decay rates, paired  $^{10}\text{Be}$  and  $^{26}\text{Al}$  of a given surface or sample can indicate whether the sample was constantly exposed since the last glacial (erosion) event, or whether the sample has a more complex history at timescales that are detectable with the  $^{26}\text{Al}/^{10}\text{Be}$  system. At the surface, the nuclides are produced at a known ratio. If a sample has been buried or covered at a sufficient depth or thickness, production of cosmogenic nuclides stops, while nuclide decay continues. The subsequent  $^{26}\text{Al}/^{10}\text{Be}$  values in that sample plot below the 'constant-exposure line' or below the 'erosion island' in an  $^{26}\text{Al}/^{10}\text{Be}$  against  $^{10}\text{Be}$  concentration plot if that shielded period lasted at least 150 ka, indicating a complex-exposure history (see Fig. 3 in the Results; Gosse and Phillips, 2001). If the sample plots on the line, the  $^{26}\text{Al}/^{10}\text{Be}$  indicates absence of long shielding periods (Brook *et al.*, 1996; Sugden *et al.*, 2005; Stone *et al.*, 1998).

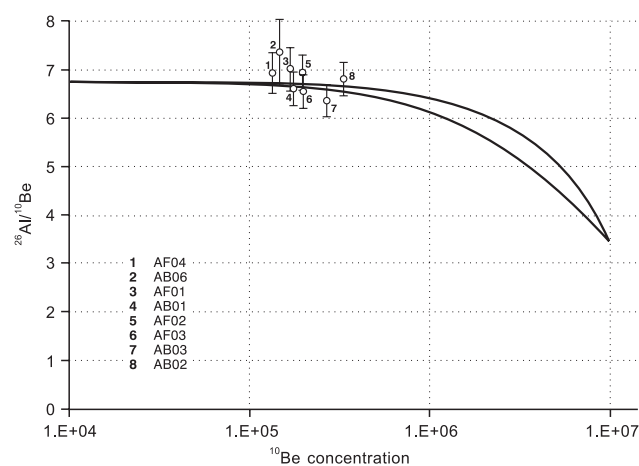


**Figure 3.** 'Banana' plot for  $^{10}\text{Be}$  and  $^{26}\text{Al}$  ages of samples collected on Aran Fawddwy and Aran Benllyn. Note that the  $^{10}\text{Be}$  and  $^{26}\text{Al}$  ages for each sample are indistinguishable and the  $^{26}\text{Al}/^{10}\text{Be}$  ratios for all samples overlap (within one-sigma uncertainty) the constant-exposure production-rate ratio line. This indicates that the samples do not have complex exposure histories detectable by the  $^{26}\text{Al}/^{10}\text{Be}$  system.

### Sample preparation for $^{10}\text{Be}$ and $^{26}\text{Al}$ analysis

Purified quartz was obtained from the 250- to 500- $\mu\text{m}$  size fraction of the crushed rocks and BeO targets were prepared for  $^{10}\text{Be}/^9\text{Be}$  analysis using the procedure described by Wilson *et al.* (2008) as modified by Glasser *et al.* (2009). Further modifications compared with Glasser *et al.* (2009) are: (1) sample preparation was also carried out for  $^{26}\text{Al}$  (see below); (2) 200  $\mu\text{g}$  Be was added as carrier and (3) about 12 g sample was dissolved. After dissolution of the sample, Al carrier was added to reach a total of 1.6 mg Al per sample. Total aluminium (native in quartz plus carrier) was determined with ICP-OES at SUERC. One-sigma uncertainties of total Al were typically 3%. The measurement procedures at the SUERC AMS are described in detail in Xu *et al.* (2010). Typical ion currents of  $^{27}\text{Al}$  were 250–420 nA. Z92-0222 (donated from PRIME Lab, Purdue University, West Lafayette, IN, USA) with a nominal  $^{26}\text{Al}/^{27}\text{Al}$  ratio of  $4.11 \times 10^{-11}$  was used as primary standard. The measurements of this material agree with the measurements of standard material supplied by K. Nishiizumi (2004). The treatment of the uncertainties that contribute to the uncertainty of the  $^{26}\text{Al}$  concentration in atoms  $\text{g}^{-1}$  quartz is described in Roberts *et al.* (2008).

### Exposure age calculations

Exposure ages were calculated using the CRONUS-Earth online calculator (Balco *et al.*, 2008) (version: wrapper script 2.2; main calculator 2.1; constants 2.2.1). The Sea-level High Latitude (SLHL) production rate (spallogenic production only) used for  $^{10}\text{Be}$  is  $4.39 \text{ atoms g}^{-1} \text{ a}^{-1}$ . The ratio of the SLHL production rates for  $^{10}\text{Be}$  and  $^{26}\text{Al}$  is 6.75. Attenuation correction for sample thickness uses an attenuation length of  $160 \text{ g cm}^{-2}$ . Topographic shielding correction is determined according to Dunne *et al.* (1999). The exposure ages are based on the time-dependent Lal/Stone scaling scheme (Lm scheme in the calculator) (Table 2). The ages resulting from this scheme are younger by about 5% than those derived from Dunai's scheme (Dunai, 2001), but about 1% older than those derived from Lifton's scheme (Lifton *et al.*, 2005) (see Table 3). The half-life of  $^{10}\text{Be}$  used is based on the new determinations by Korschinek *et al.* (2010) and Chmeleff *et al.* (2010) whilst the half-life of  $^{26}\text{Al}$  is based on Norris *et al.* (1983) and Middleton *et al.* (1983). The relative internal uncertainty of the exposure ages is equivalent to the relative uncertainty of the radionuclide concentration. The external uncertainty also includes the uncertainty of the production rate.  $^{10}\text{Be}$  and  $^{26}\text{Al}$  analyses can be used to test for complex exposure and shielding histories at long time-scales, such as on high-elevation sites above trimlines (Gosse and Phillips, 2001). We assume zero erosion

rates as seven samples were taken from resistant quartz veins and one sample was taken from a resistant rhyolitic vein.

## Results

### Geomorphological mapping

Geomorphological mapping from aerial photographs and fieldwork indicate that the ridge between Aran Fawddwy and Aran Benllyn was entirely ice-covered and overridden by ice at some point during the Pleistocene (Figs 1 and 2). There is evidence of ice overriding and glacial erosion in the form of ice-moulded bedrock forms on all parts of the ridge. Ice-moulded lee and fractured stoss bedrock faces indicate that ice moved over the Aran ridge from a north-westerly direction. Ice-moulded bedrock landforms are present even as high as the summit of Aran Fawddwy at 905 m a.s.l., and the summit of Aran Benllyn at 885 m a.s.l. (Figs 1 and 2B).

Geomorphological mapping indicates that there are two types of ice-moulded bedrock on the main ridge: ice-moulded bedrock landforms at lower elevations with a fresh surface appearance (Fig. 2D) and more degraded ice-moulded bedrock landforms at higher elevations with varying degrees of frost-shattering developed on their upper surfaces (Fig. 2C). This transition is not like a sharp trimline observed on other mountains in Wales (cf. McCarroll and Ballantyne, 2000). There is no clear altitudinal boundary between these two types of ice moulding; rather there is a gradual transition around altitudes of 750–800 m a.s.l. (Hughes, 2002a). Above this altitude frost-shattering is widespread unlike at lower altitudes, although well-preserved ice-moulded bedrock is not exclusive

to the lower slopes and occurs in isolated areas even close to the highest parts of the ridge (Figs 1 and 2B).

It is possible that the two types of ice moulding are approximately the same age but the difference in their appearance represents different stages of weathering of an initially ice-scoured bedrock surface. Varying degrees of frost shattering may be controlled by differences in bedrock joint density on the summits above 750–800 m a.s.l. compared with the lower slopes. However, on geological maps the entire ridge crest ranging from 300 to 905 m is formed in the same felsic tuffs. Given the limited altitudinal variation of these mountains, strong variations in frost-shattering with altitude are unlikely.

It is also possible that the two types of ice moulding represent two different, time-separated, ice overriding events. In this scenario the more degraded ice-moulded surfaces at higher elevations would therefore be expected to be of greater antiquity than the fresher ice-moulded surfaces at lower altitudes. This possibility can be tested by applying <sup>10</sup>Be and <sup>26</sup>Al to date the different bedrock surfaces.

### <sup>10</sup>Be and <sup>26</sup>Al dating of bedrock surfaces on the Aran ridge

Eight samples were collected and analysed (Tables 1–3): two samples on ice-moulded bedrock below 750–800 m a.s.l. and six samples on ice-moulded bedrock above 750–800 m a.s.l. The six samples above 750–800 m a.s.l. yielded paired <sup>10</sup>Be and <sup>26</sup>Al ages ranging from 17.5 ± 0.6/17.2 ± 0.6 to 33.9 ± 1.2/34.4 ± 1.3 ka. Four of these samples are close in age (<sup>10</sup>Be ages of 17.5 ± 0.6, 17.5 ± 0.7, 19.7 ± 0.8 and

**Table 2.** <sup>10</sup>Be and <sup>26</sup>Al concentrations and related exposure ages of samples from Aran Fawddwy and Aran Benllyn.

Sample*	<sup>10</sup> Be, <sup>26</sup> Al SUERC AMS ID	Blank-corrected <sup>10</sup> Be ± uncertainty (10 <sup>5</sup> at g <sup>-1</sup> ) <sup>†</sup>	<sup>10</sup> Be age (ka) <sup>‡</sup>	Internal uncertainty on <sup>10</sup> Be age (ka) <sup>§</sup>	External uncertainty on <sup>10</sup> Be age (ka) <sup>§</sup>	Blank-corrected <sup>26</sup> Al ± uncertainty (10 <sup>5</sup> at g <sup>-1</sup> ) <sup>¶</sup>	<sup>26</sup> Al age (ka) <sup>‡</sup>	Internal uncertainty on <sup>26</sup> Al age (ka) <sup>§</sup>	External uncertainty on <sup>26</sup> Al age (ka) <sup>§</sup>	<sup>26</sup> Al/ <sup>10</sup> Be
AB01	b4258, a1238	1.752 ± 0.064	17.51	0.63	1.61	11.61 ± 0.43	17.17	0.64	1.60	6.63 ± 0.35
AB02	b4261, a1239	3.317 ± 0.118	33.93	1.20	3.13	22.62 ± 0.86	34.38	1.31	3.23	6.82 ± 0.35
AB03	b4262, a1240	2.676 ± 0.095	27.50	0.97	2.53	17.08 ± 0.64	26.02	0.96	2.43	6.38 ± 0.33
AF01	b4644, a1241	1.682 ± 0.064	17.54	0.65	1.63	11.82 ± 0.62	18.26	0.94	1.83	7.03 ± 0.45
AF02	b4264, a1244	1.951 ± 0.072	19.95	0.73	1.84	13.56 ± 0.51	20.53	0.77	1.92	6.95 ± 0.37
AF03	b4265, a1245	1.979 ± 0.077	19.72	0.75	1.84	12.98 ± 0.47	19.15	0.70	1.78	6.56 ± 0.35
AB06	b4642, a1342	1.455 ± 0.067	18.37	0.84	1.77	10.72 ± 0.83	20.03	1.54	2.32	7.37 ± 0.67
AF04	B4267, a1246	1.335 ± 0.061	16.54	0.75	1.59	9.282 ± 0.361	17.01	0.66	1.59	6.95 ± 0.42

Exposure ages are based on the time-dependent Lal/Stone scheme (Lm) (Balco *et al.*, 2008; wrapper script 2.2; main calculator 2.1; constants 2.2.1). This means that the production rates are corrected for their variation with time. Samples AB01–AF03 were collected from degraded ice-moulded bedrock at sites >750–800 m a.s.l. whilst samples AB06 and AF04 were collected from well-preserved ice-moulded bedrock on the lower parts of the ridge at altitudes of <750–800 m a.s.l. All reported uncertainties are 1σ. The topographic shielding factor for all samples is 1.0, meaning that none of the samples were shielded by any topography.

\*All but one sample was collected from quartz veins exposed on the surfaces of exposed bedrock (see Table 1). Sample AB06 was collected from a quartz-rich fine- to medium-grained rhyolite vein.

<sup>†</sup>Blank-corrected <sup>10</sup>Be concentrations that are standardized to the primary AMS standard NIST SRM4325 with a <sup>10</sup>Be/<sup>9</sup>Be ratio of 2.79 × 10<sup>-11</sup> (Nishiizumi *et al.*, 2007). Nishiizumi's <sup>10</sup>Be determination in NIST SRM4325 is independent of the half-life of <sup>10</sup>Be. Values are not corrected for total physical shielding. Uncertainty includes the uncertainty of: (1) the sample measurement on the SUERC AMS; (2) the process-blank correction; and (3) the chemical sample preparation, which includes the uncertainty of the Be concentration in the carrier solution. Fully processed blanks had an average <sup>10</sup>Be/<sup>9</sup>Be ratio of 6.0 × 10<sup>-15</sup>, which was subtracted from the <sup>10</sup>Be/<sup>9</sup>Be ratio of the samples, which ranged from 1.3 to 3.3 × 10<sup>-13</sup>.

<sup>‡</sup>All exposure ages were calculated using the time-dependent Lal (1991)/Stone (2000) scaling scheme in the Balco *et al.* (2008) CRONUS-Earth online calculator (version 2.2) (<http://hess.ess.washington.edu/>). A density of 2.65 g cm<sup>-3</sup> and the standard atmospheric pressure–elevation relationship were used in the calculations.

<sup>§</sup>Uncertainties of exposure ages and <sup>26</sup>Al/<sup>10</sup>Be ratios include the uncertainty in production rates.

<sup>¶</sup>Blank-corrected <sup>26</sup>Al concentrations that are standardized to the 705-ka <sup>26</sup>Al half-life of Middleton *et al.* (1983). Values are not corrected for total physical shielding. Uncertainty includes the uncertainty of: (1) the sample measurement on the SUERC AMS; (2) the process-blank correction; and (3) the chemical sample preparation, which includes the uncertainty of the Be concentration in the carrier solution. Fully processed blanks had an average <sup>26</sup>Al/<sup>27</sup>Al ratio of 1.2 × 10<sup>-15</sup>, which was subtracted from the <sup>26</sup>Al/<sup>27</sup>Al ratio of the samples, which ranged from 3.2 to 7.5 × 10<sup>-13</sup>. The primary <sup>26</sup>Al standard (Z92-0222) with a nominal <sup>26</sup>Al/<sup>27</sup>Al ratio of 4.11 × 10<sup>-11</sup> was used for normalization. This normalization is in agreement with K. Nishiizumi's <sup>26</sup>Al standard material (Nishiizumi *et al.*, 2007).

**Table 3.**  $^{10}\text{Be}$  and  $^{26}\text{Al}$  exposure ages of samples from ice-moulded bedrock surfaces on Aran Benllyn (AB) and Aran Fawddwy (AF) calculated with the time-independent Lal (1991)/Stone (2000) scaling scheme (using production rates that average over the last c. 10 ka), as well as the time-dependent scaling schemes of Desilets and Zreda (2003), (2006), Dunai (2001) and Lifton *et al.* (2005).

Sample ID	Lal (1991)/Stone (2000)		Desilets <i>et al.</i> (2003, 2006)		Dunai (2001)		Lifton <i>et al.</i> (2005)	
	$^{10}\text{Be}$ age (ka)	Internal uncertainty on $^{10}\text{Be}$ age (ka)	$^{10}\text{Be}$ age (ka)	External uncertainty on $^{10}\text{Be}$ age (ka)	$^{10}\text{Be}$ age (ka)	External uncertainty on $^{10}\text{Be}$ age (ka)	$^{10}\text{Be}$ age (ka)	External uncertainty on $^{10}\text{Be}$ age (ka)
AB01	17.20	1.63	18.23	2.26	18.36	2.27	17.47	1.84
AB02	33.42	3.16	35.36	4.39	35.44	4.39	33.60	3.55
AB03	27.06	2.56	28.66	3.55	28.77	3.55	27.30	2.88
AF01	17.23	1.64	18.28	2.28	18.41	2.28	17.53	1.86
AF02	19.60	1.86	20.77	2.58	20.90	2.59	19.86	2.10
AF03	19.38	1.85	20.52	2.56	20.65	2.57	19.62	2.09
AB06	16.24	1.60	19.17	2.44	19.31	2.45	18.42	2.01
AF04	17.20	1.63	17.27	2.19	17.41	2.20	16.62	1.81

20.0 ± 0.7 ka) while two are much older (27.5 ± 1.0 and 33.9 ± 1.2 ka).

Concentrations of cosmogenic  $^{10}\text{Be}$  and  $^{26}\text{Al}$  in the ice-moulded bedrock landforms were used to establish the exposure history (complex or simple) and to determine the timing of ice overriding and glacial erosion. The paired-nuclide approach was adopted because it is possible that the bedrock surfaces have a complex exposure history. In the past, bedrock surfaces could have possibly been covered by more than one ice cap, with re-exposure in between, and also possibly been covered by non-erosive cold-based, protective ice. The paired-nuclide approach can test this possibility, unlike a single nuclide (typically  $^{10}\text{Be}$ ) approach (cf. Miller *et al.*, 2006; Bentley *et al.*, 2006). This is particularly important in the case of our highest summit samples where there is the possibility of cold-based ice coverage. However, plots of our  $^{26}\text{Al}/^{10}\text{Be}$  ratios versus  $^{10}\text{Be}$  concentrations show that all exposure ages agree within a one-sigma error range with the production rate ratio line, and there is approximate concordance in  $^{26}\text{Al}$  and  $^{10}\text{Be}$  ages (Fig. 3). This indicates that there is no evidence for complex exposure history in our samples and the summits of the Arans have remained exposed – and not covered by cold-based ice – after the last phase or glacial erosion.

Note that the two older outliers also do not show any evidence of burial in the  $^{26}\text{Al}$  and  $^{10}\text{Be}$  data and display similar  $^{26}\text{Al}$  and  $^{10}\text{Be}$  ages (26.0 ± 1.0/27.5 ± 1.0 and 34.4 ± 1.3/33.9 ± 1.2 ka). It is possible that these old outliers represent minimum real exposure ages, with a previous exposure history component in those ages that contributes to their total  $^{26}\text{Al}$  and  $^{10}\text{Be}$  concentrations. On the balance of evidence, with the six other samples yielding much younger closely clustered ages the two older outliers are considered here to be ‘anomalously’ old.

## Discussion

The paired-nuclide approach allows us to test the hypothesis that the Aran ridge was not overrun by ice during the LGM and, instead, the summits stood above the ice as nunataks at this time. Six of the eight  $^{26}\text{Al}$  and  $^{10}\text{Be}$  data indicate that ice-moulded bedrock was exposed after 20 ka. However, two of the paired  $^{10}\text{Be}/^{26}\text{Al}$  ages from the Aran ridge are older (c. 27 and 34 ka) than the four others (tightly grouped between c. 17 and 20 ka). The simplest explanation is that the two older ages contain inheritance because glacial erosion has not removed sufficient bedrock (c. 2 m) to zero the cosmogenic nuclide signal. These two samples are both from large quartz outcrops on the summit ridge which may represent resistant bedrock

obstacles with an inherited cosmogenic nuclide signal (Fig. 2A). As noted earlier, this is the most reasonable interpretation based on the balance of evidence and future cosmogenic exposure-age dating of neighbouring mountain summits in this area will help further test the interpretations made here. Thus, based on the majority of the data, the hypothesis that the Arans stood above the Welsh Ice Cap during the LGM (Hughes, 2002a, b) can be rejected. The data largely support the argument that ice overran the Arans during the LGM (cf. McCarroll and Ballantyne, 2002). However, the results of this study cannot determine when ice was at its thickest and this may have occurred before the LGM.

Although there is potential evidence of inherited nuclides in samples AB02 and AB03, which yield anomalously old ages, there is no evidence of a complex exposure history. The  $^{10}\text{Be}$  and  $^{26}\text{Al}$  results from the Aran ridge indicate that all samples plot on the constant-exposure line (Lal, 1991) and yield similar exposure ages (within one-sigma error). Thus, it is clear that more than 2 m of bedrock was eroded from the summit ridge by warm-based ice before being exposed in the Late Devensian.

Lower elevation ice-moulded bedrock landforms (below 750–800 m a.s.l.) yield cosmogenic isotope ages of 16.5 and 18.4 ka. During ice down-wastage it is to be expected that the Arans stood as nunataks for some period of time. However, the difference in the ages of the bedrock surfaces above and below 750–800 m a.s.l. are not large and given the errors associated with these ages it is not clear how long the Aran summits stood above the Welsh Ice Cap as nunataks. Clark *et al.* (2010) suggest that most of the Welsh Ice Cap would have disappeared by 16 ka, which is supported by the lowest altitude exposure age of 16.5 ka from the Arans. This implies that the Arans would have stood as nunataks for only a few thousand years in the period between 20 and 16 ka. Nevertheless, the period between 17 and 16 ka corresponds with Heinrich Event 1, a well-known period of enhanced ice-rafting and cooling of surface waters in the North Atlantic. It is clear from the results presented in this paper that the summits of the Aran ridge were exposed during Heinrich Event 1. This cold event would have caused marked subaerial frost-shattering at a time when lower slopes and valleys remained glaciated.

The exposure of the summits of the Arans after 20 ka corresponds to the timing of retreat of Irish Sea ice around Wales. In north-east Wales, Rowlands (1971) dated mammoth remains in a cave near Tremierchion to 18.0 ± 1.4  $^{14}\text{C}$  ka BP (21.6 ± 1.6 cal ka BP). As these caves are claimed to have been sealed by till, this age provides a maximum limiting age for the

extent of Irish Sea ice at the Bodfari–Trefnant moraine in the Vale of Clwyd. In north-west Wales, McCarroll *et al.* (2010) presented <sup>10</sup>Be exposure ages from Anglesey and the Llyn Peninsula in the range 17.7–23.6 ka.

Unlike for the Irish Sea ice sheet and other parts of the BIIS, there is little geochronological evidence for the timing of the maximum extent of the Welsh Ice Cap (Chiverell and Thomas, 2010). However, there is good control on the timing of deglaciation. For example, ice had retreated from the lower valleys of Cadair Idris, just 15 km west of the Arans, by  $13.2 \pm 0.1$  <sup>14</sup>C ka BP (Lowe, 1981) ( $16.1 \pm 0.4$  cal ka BP). This age is consistent with exposure of the lower parts of the Aran ridge shortly before, at 16.5 ka. Our new data on the former vertical extent of the Welsh Ice Cap can be linked to larger debates regarding the upper limits of the Welsh Ice Cap and the timing of different phases of landform development beneath this part of the BIIS (Hughes, 2002a,b; McCarroll and Ballantyne, 2002). For example, Jansson and Glasser (2005) suggested that during deglaciation the Welsh Sector of the BIIS was drained by a series of fast-flowing outlet glaciers. The exposure-age data presented here confirm that this is the case, with glacial erosion restricted to the lower slopes of mountain ranges such as the Arans.

McCarroll and Ballantyne (2000) proposed a thin ice sheet over the mountains of northern Snowdonia with an upper ice limit at c. 850 m a.s.l. On Cadair Idris, 15–20 km to the south-west of the Aran ridge, there is clear evidence for intense frost shattering and prolonged weathering on the summit ridges and Ballantyne (2001) suggested that the surface of the last ice sheet in this area was situated at an altitude of c. 750 m a.s.l. In the Arans, here we have shown that the upper limit of the Welsh Ice Cap was situated at an altitude of at least 900 m, and given the erosion that occurred over the summits, the ice cap surface is likely to have been significantly higher. However, as the summits of the Aran ridge were glaciated by ice moving from the north-west to the south-west, then the ice surface must have been even higher over the mountains of Rhobell Fawr and Dduallt in the Arenigs immediately to the north-west of the Arans (Fig. 1). This supports the ideas of Greenly (1919) who suggested that the centre of the last Welsh Ice Cap was positioned between the Rhinogs and the Arenigs.

Further work is required to test whether the mountains of northern Snowdonia and Cadair Idris did indeed stand above the LGM ice sheet as nunataks or whether the intense frost shattering and preservation of long-term weathering products in the soils on these summits was preserved under cold-based ice at the LGM. Further work is also required in order to establish the exposure histories of mountains surrounding the postulated ice centre of Greenly (1919), including the Rhinogs and the Arenigs (Fig. 1). This will ultimately enable a better understanding of the surface geometry of the last Welsh Ice Cap and the timing of ice cap retreat.

## Conclusions

The paired cosmogenic isotopes from the eight samples collected on ice-moulded bedrock landforms along the Aran ridge indicate that the summits were exposed at c. 20 ka, soon after complete ice coverage and glacial erosion of the mountains at the LGM (26–21 ka). These results indicate that the Welsh Ice Cap was thick enough in this area to submerge the mountains of both Aran Fawddwy (905 m a.s.l.) and Aran Benllyn (885 m a.s.l.) during the Devensian. The ice cap was also able to achieve glacial erosion at high elevations on these summits. It is likely that the summits were exposed as nunataks between c. 20 and 17 ka when the lower slopes were still ice-covered. During this interval a phase of intense glaciation

continued at lower altitudes, characterized by large outlet glaciers in the valleys separated by nunataks.

**Acknowledgements.** This work was supported by a UK Natural Environment Research Council (NERC) Award through the NERC Cosmogenic Isotope Analysis Facility (CIAF allocation 9069.1009). Allan Davidson at SUERC performed the chemistry and target preparation. Graham Bowden in the School of Environment and Development at the University of Manchester drew Fig. 3. We would like to thank Colin Ballantyne and Glenn Thackray for very useful comments on this paper.

**Abbreviations.** BIIS, British–Irish Ice Sheet; LGM, Last Glacial Maximum; SLHL, Sea-level High Latitude.

## References

- Balco G, Stone JO, Lifton NA, *et al.* 2008. A complete and easily accessible means of calculating surface exposure ages or erosion rates from <sup>10</sup>Be and <sup>26</sup>Al measurements. *Quaternary Geochronology* **3**: 174–195.
- Ballantyne CK. 2001. Cadair Idris: a Late Devensian palaeonunatak. In Walker MJC, McCarroll D (eds), *The Quaternary of West Wales: Field Guide*. Quaternary Research Association: London; 126–131.
- Ballantyne CK. 2010. Extent and deglacial chronology of the last British–Irish Ice Sheet: implications of exposure dating using cosmogenic isotopes. *Journal of Quaternary Science* **25**: 515–534.
- Bentley MJ, Fogwill CJ, Kubik PW, *et al.* 2006. Geomorphological evidence and cosmogenic <sup>10</sup>Be/<sup>26</sup>Al exposure ages for the Last Glacial Maximum and deglaciation of the Antarctic Peninsula Ice Sheet. *Geological Society of America Bulletin* **118**: 1149–1159.
- Bowen DQ. 1973. The Pleistocene history of Wales and the borderland. *Geological Journal* **8**: 207–224.
- Bowen DQ, Phillips FM, McCabe AM, *et al.* 2002. New data for the Last Glacial Maximum in Great Britain and Ireland. *Quaternary Science Reviews* **21**: 89–101.
- Brook EJ, Nesje A, Lehman S, *et al.* 1996. Cosmogenic exposure ages along a vertical transect in western Norway: implications for the height of the Fennoscandian Ice Sheet. *Geology* **24**: 207–210.
- Chmeleff J, von Blanckenburg F, Kossert K, *et al.* 2010. Determination of the <sup>10</sup>Be half-life by multicollector ICP-MS and liquid scintillation counting. *Nuclear Instruments and Methods in Physics Research B* **268**: 192–199.
- Chiverell RC, Thomas GSP. 2010. Extent and timing of the Last Glacial Maximum (LGM) in Britain and Ireland: a review. *Journal of Quaternary Science* **25**: 535–549.
- Clark CD, Hughes ALC, Greenwood SL, *et al.* 2010. Pattern and timing of retreat of the last British–Irish Ice Sheet. *Quaternary Science Reviews* (in press) [doi: 10.1016/j.quascirev.2010.07.019].
- Cockburn HAP, Summerfield MA. 2004. Geomorphological applications of cosmogenic isotope analysis. *Progress in Physical Geography* **28**: 1–42.
- Desilets D, Zreda M. 2003. Spatial and temporal distribution of secondary cosmic-ray nucleon intensities and applications to in-situ cosmogenic dating. *Earth and Planetary Science Letters* **206**: 21–42.
- Desilets D, Zreda M, Prabu T. 2006. Extended scaling factors for in situ cosmogenic nuclides: New measurements at low latitude. *Earth and Planetary Science Letters* **246**: 265–276.
- Dunai TJ. 2001. Influence of secular variation of the magnetic field on production rates of in situ produced cosmogenic nuclides. *Earth and Planetary Science Letters* **176**: 157–169.
- Dunne J, Elmore D, Muzikar P. 1999. Scaling factors for the rates of production of cosmogenic nuclides for geometric shielding and attenuation at depth on sloped surfaces. *Geomorphology* **27**: 3–11.
- EDINA Geology Digimap. 2009. British Geological Survey (BGS) data. <http://edina.ac.uk/digimap/index.shtml>
- Eyles N, McCabe AM. 1989. The Late Devensian (<22,000 BP) Irish Sea basin: the sedimentary record of a collapsed ice sheet margin. *Quaternary Science Reviews* **8**: 307–351.
- Fearnside WG. 1905. On the Geology of Arenig Fawr and Moel Llyfnant. *Quarterly Journal of the Geological Society* **61**: 608–640.
- Glasser NF, Hambrey MJ, Huddart D, *et al.* 2001. Terrestrial glacial sedimentation on the eastern margin of the Irish Sea basin: Thurstaston, Wirral. *Proceedings of the Geologists Association* **112**: 131–146.

- Glasser NF, Clemmens S, Schnabel C, *et al.* 2009. Tropical glacier advances in the Cordillera Blanca, Peru between 12.5 and 7.6 ka from cosmogenic  $^{10}\text{Be}$  dating. *Quaternary Science Reviews* **28**: 3448–3458.
- Greenly E. 1919. *The Geology of Anglesey*. Memoirs of the Geological Survey of Great Britain, HMSO: London.
- Gosse JC, Phillips FM. 2001. Terrestrial in situ cosmogenic nuclides: theory and application. *Quaternary Science Reviews* **20**: 1475–1560.
- Hubbard A, Bradwell T, Golledge N, *et al.* 2009. Dynamic cycles, ice streams and their impact on the extent, chronology and deglaciation of the British–Irish Ice Sheet. *Quaternary Science Reviews* **28**: 758–776.
- Hughes PD. 2002a. Nunataks and the surface altitude of the last ice-sheet in southern Snowdonia, Wales. *Quaternary Newsletter* **97**: 19–25.
- Hughes PD. 2002b. Nunataks and the surface altitude of the last ice-sheet in southern Snowdonia, Wales: a reply to McCarroll and Ballantyne (2002). *Quaternary Newsletter* **98**: 15–17.
- Hughes PD. 2002c. Loch Lomond Stadial glaciers in the Aran and Arenig Mountains, North Wales, Great Britain. *Geological Journal* **37**: 9–15.
- Hughes PD. 2009. Loch Lomond Stadial (Younger Dryas) glaciers and climate in Wales. *Geological Journal* **44**: 375–391.
- Jansson KN, Glasser NF. 2005. Palaeoglaciology of the Welsh sector of the British–Irish Ice Sheet. *Journal of the Geological Society, London* **162**: 25–37.
- Korschinek G, Bergmaier A, Faestermann T, *et al.* 2010. A new value for the half-life of  $^{10}\text{Be}$  by heavy-ion elastic recoil detection and liquid scintillation counting. *Nuclear Instruments and Methods in Physics Research B* **268**: 187–191.
- Lal D. 1991. Cosmic ray labelling or erosion surfaces: *in situ* nuclide production rates and erosion models. *Earth and Planetary Science Letters* **104**: 424–439.
- Lifton N, Bieber J, Clem J, *et al.* 2005. Addressing solar modulation and long-term uncertainties in scaling secondary cosmic rays for in situ cosmogenic nuclide applications. *Earth and Planetary Science Letters* **239**: 140–161.
- Lowe S. 1981. Radiocarbon dating and stratigraphic resolution in Welsh lateglacial chronology. *Nature* **293**: 201–212.
- MARGO Project Members. 2009. Constraints on the magnitude and patterns of ocean cooling at the Last Glacial Maximum. *Nature Geoscience* **2**: 127–132.
- McCarroll D. 2001. Deglaciation of the Irish Sea Basin: a critique of the glaciomarine hypothesis. *Journal of Quaternary Science* **16**: 393–404.
- McCarroll D, Ballantyne CK. 2000. The last ice sheet in Snowdonia. *Journal of Quaternary Science* **15**: 765–778.
- McCarroll D, Ballantyne CK. 2002. Nunataks and the surface altitude of the last ice-sheet in southern Snowdonia, Wales: a comment on Hughes (2002). *Quaternary Newsletter* **98**: 10–14.
- McCarroll D, Stone SO, Ballantyne CK, *et al.* 2010. Exposure-age constraints on the extent, timing and rate of retreat of the last Irish Sea ice stream. *Quaternary Science Reviews* **29**: 1844–1852.
- Middleton R, Klein J, Raisbeck GM, *et al.* 1983. Accelerator Mass Spectrometry with  $^{26}\text{Al}$ . *Nuclear Instruments, Methods and Physics Research* **218**: 430.
- Miller GH, Briner JP, Lifton NA, *et al.* 2006. Limited ice-sheet erosion and complex exposure histories derived from in situ cosmogenic  $^{10}\text{Be}$ ,  $^{26}\text{Al}$ , and  $^{14}\text{C}$  on Baffin Island, Arctic Canada. *Quaternary Geochronology* **1**: 74–85.
- Mix AC, Bard E, Schneider R. 2001. Environmental processes of the ice age: land, oceans, glaciers (EPILOG). *Quaternary Science Reviews* **20**: 627–657.
- Nishiizumi K. 2004. Preparation of  $^{26}\text{Al}$  AMS standards. *Nuclear Instruments and Methods in Physics Research B* **223–224**: 388–392.
- Nishiizumi K, Imamura M, Caffee MW, *et al.* 2007. Absolute calibration of  $^{10}\text{Be}$  AMS standards. *Nuclear Instruments and Methods in Physics Research B* **258**: 403–413.
- Norris TL, Gancarz AJ, Rokop DJ, *et al.* 1983. Half-life of  $^{26}\text{Al}$ . *Journal of Geophysical Research* **88**: B331.
- O’Cofaigh C, Evans DJA. 2001. Deforming bed conditions associated with a major ice stream of the last British ice sheet. *Geology* **29**: 795–798.
- O’Cofaigh C, Evans DJA. 2007. Radiocarbon constraints on the age of the maximum advance of the British–Irish Ice Sheet in the Celtic Sea. *Journal of Quaternary Science* **26**: 1197–1203.
- Peltier WR, Fairbanks RG. 2006. Global glacial ice volume and Last Glacial Maximum duration from an extended Barbados sea level record. *Quaternary Science Reviews* **26**: 862–875.
- Roberts DH, Long AJ, Schnabel C, *et al.* 2008. The deglacial history of the southeast sector of the Greenland Ice Sheet during the Last Glacial Maximum. *Quaternary Science Reviews* **27**: 1505–1516.
- Rowlands BM. 1971. Radiocarbon evidence of the age of an Irish Sea glaciation in the Vale of Clwyd. *Nature-Physical Science* **230**: 9–11.
- Stone JO, Ballantyne CK, Fifield LK. 1998. Exposure dating and validation of periglacial weathering limits, northwest Scotland. *Geology* **26**: 587–590.
- Stone JO. 2000. Air pressure and cosmogenic isotope production. *Journal of Geophysical Research* **105**(B10): 23753–23759.
- Sugden DE, Balco G, Cowdery SG, *et al.* 2005. Selective glacial erosion and weathering zones in the coastal mountains of Marie Byrd Land, Antarctica. *Geomorphology* **67**: 317–334.
- Thomas GSP. 1985. The Late Devensian glaciation along the border of northeast Wales. *Geological Journal* **20**: 319–340.
- Wilson P, Bentley M, Schnabel C, *et al.* 2008. Stone run (block stream) formation in the Falkland Islands over several cold stages, deduced from cosmogenic isotope ( $^{10}\text{Be}$  and  $^{26}\text{Al}$ ) surface exposure dating. *Journal of Quaternary Science* **23**: 461–473.
- Yokoyama Y, Lambeck K, DeDeckker P, *et al.* 2000. Timing of the Last Glacial Maximum from observed sea-level minima. *Nature* **406**: 713–716.
- Xu S, Dougans AB, Freeman SPHT, *et al.* 2010. Improved  $^{10}\text{Be}$  and  $^{26}\text{Al}$  AMS with a 5 MV spectrometer. *Nuclear Instruments and Methods in Physics Research B* **268**: 736–738.